Differential gain and damping factor in strained InGaAs/GaAs quantum well lasers

L. F. Lester, W. J. Schaff, S. S. O'Keefe, X. Song, B. A. Foreman, and L. F. Eastman

School of Electrical Engineering and the National Nanofabrication Facility
Cornell University
Ithaca, NY 14853

ABSTRACT

The differential gain, modulation response, and damping rate of strained-layer $In_{0.3}Ga_{0.7}As$ multiple quantum well (MQW) short cavity graded-index separate confinement heterostrucutre (GRINSCH) and SCH lasers fabricated by chemically-assisted ion beam etching (CAIBE) are analyzed. Calculated differential gains vary from 0.7 to 1.6 x 10^{-15} cm^2, with only relatively long lasers of 400 μm demonstrating very high differential gain. For the GRINSCH lasers, a CW 3-dB bandwidth of 22 GHz has been measured that is limited primarily by heating and a low frequency rolloff. The latter is improved dramatically using an SCH design resulting in an improvement of the 3-dB bandwidth to 28 GHz. Carrier transport theory (also known as well-barrier hole burning) is shown to model the damping behavior of quantum well lasers from low to moderate photon densities.

1. INTRODUCTION

Both theoretical calculations and experimental data have shown that the increased differential gain in strained-layer $In_xGa_{1-x}As$ quantum well (QW) lasers makes them faster than GaAs QW lasers[1,2]. A five quantum well structure containing 50 Å $In_{0.3}Ga_{0.7}As$ layers with GaAs barriers has demonstrated an extremely high differential gain of 2.1 x 10^{-15} cm^2 in a 200 μm cavity length laser[3]. This factor of seven improvement in differential gain over that of bulk, p-type doped InGaAsP lasers[4] clearly shows the potential of strained-layer quantum well (SLQW) lasers for very high modulation bandwidths. Thus, the development of SLQW lasers with 3-dB bandwidths from 16.5-23.5 GHz has been rapid[5,6,7,8]. To date, GaAs-based strained layer devices have a slight edge in reported 3-dB bandwidths, but lasers from both material systems have demonstrated very low K-factors from 0.13-0.22 ns[6,7,8,9]. These numbers indicate that intrinsic maximum 3-dB bandwidths from 40-68 GHz are possible.

At the same time, damping in QW lasers must be considered to ensure that the improvement in RF bandwidth from the increased differential gain in SLQW structures is not nullified by a very high non-linear gain coefficient, ε. Published values of ε in QW lasers have varied widely. Some reported ε's are as low as those of bulk lasers (about 1 x 10^{-17} cm^3)[10] while other numbers are anomalously high (about 5.7-7.55 x 10^{-17} cm^3)[11,12,13,14]. Although the exact cause of these differences is not clear, several structure dependent theories have been proposed to explain the wide variation in ε. These models, which include carrier heating[15], spectral hole burning[16], and carrier transport effects[11,17,18], indicate that gain saturation in QW lasers may depend heavily on quantum well depth and thickness, barrier thickness, and well number.

In addition to structures with high differential gain, it is well known that short cavity length multiple quantum well (MQW) lasers exhibit higher frequency response by virtue of a shorter photon cavity lifetime[19]. Running a laser at a large optical power also increases the bandwidth, but the practical application of this technique is limited by either catastrophic optical damage or device heating. The latter statement implies that a low threshold current density is desirable in a high speed laser in order to minimize the bias current density, and, therefore, the device heating at a given optical power. In this work, the differential gain and damping in short cavity length graded-index separate confinement heterostructure (GRINSCH) and SCH MQW strained-layer $In_{0.3}Ga_{0.7}As/GaAs$ ridge waveguide lasers are discussed. These devices will demonstrate that very low damping rates and large modulation bandwidths are attainable in short cavity SLQW lasers. It will shown, however, that the differential gain is only very high in the relatively long cavity length lasers.

2. MATERIALS AND FABRICATION

Two GRINSCH layers were grown, the only difference being that one had a four QW (4QW) active region and the other had a five QW (5QW) active region. The following is a brief description of the layers: 1) a 1 μm GaAs n^+ buffer, a 0.15 μm n-type region graded to $Al_{0.7}Ga_{0.3}As$, and 0.45 μm n-$Al_{0.7}Ga_{0.3}As$ lower cladding region, 2) a GRINSCH active region consisting of an undoped 0.25 μm $Al_xGa_{1-x}As$ layer graded from x = 0.7 to x = 0.3, four or five undoped 50 Å $In_{0.3}Ga_{0.7}As$ quantum wells with undoped 250 Å GaAs barrier layers, and an undoped 0.25 μm $Al_xGa_{1-x}As$ layer graded from x = 0.3 to x = 0.7, 3) a 0.45 μm p-$Al_{0.7}Ga_{0.3}As$ upper cladding region, a 0.15 μm p-type layer graded to GaAs, and a 0.1 μm p^+ GaAs cap. In addition, a 4QW SCH structure with the same active region as the 4QW GRINSCH material was grown for comparison. The SCH layer consists of a 0.2 μm wide optical confinement region with 0.81 μm p^+ and n^+ $Al_{0.7}Ga_{0.3}As$ cladding regions both doped at 2×10^{18} cm^{-3}. The quantum well gain region of four 50 Å $In_{0.3}Ga_{0.7}As$ layers bounded by 250 Å GaAs barriers is centered within the optical confinement area. As in the GRINSCH layers, a 1.0 μm n^+ GaAs buffer and a 0.12 μm p^+ GaAs cap are used for the n and p-type ohmic contact layers, respectively, and highly-doped graded 0.15 μm $Al_xGa_{1-x}As$ layers (x varies from 0 to 0.7) are employed between both the cap layer/p-cladding and buffer/n-cladding regions.

With this material, ridge waveguide lasers were made using a chemically-assisted ion beam etching (CAIBE) technique to form both the ridge and mirrors of the lasers. The CAIBE method that has been developed is thermally assisted and has demonstrated a highly reproducible etch rate[20]. The ridge is etched to the top of the graded-index region, and the mirrors are etched in a subsequent step to the top of the n-type buffer layer. Ni/AuGe/Ag/Au and Ti/Pd/Au metallizations are used for the n-type and p-type ohmic contacts, respectively. The p-type contact covers only the ridge itself. Although this narrow metallization limits the spreading of heat away from the laser, the parasitic capacitance is minimized in this device configuration. All exposures are defined by electron beam lithography to improve fabrication tolerances and to improve the turn-around time of pattern alterations. The device layout is compatible with coplanar waveguide probing, which enables rapid testing of many devices while removing the parasitic capacitance and inductance associated with chip packaging[2]. With coplanar probing, metal stripes as narrow as 3 μm can be contacted. The etched mirror MQW lasers made using the process above typically emit at a wavelength of about 1.02 μm[5,20]. Devices with lengths between 50 and 400 μm and widths of 3 and 5 μm were fabricated on the various materials.

3. DIFFERENTIAL GAIN AND RF RESULTS

The relaxation oscillation frequency (or resonance frequency) as a function of bias current above threshold was measured using an HP 8131A pulse generator with a 200 ps risetime and a 1 ns pulse width, a 40 GHz bandwidth New Focus model 1012 long-wavelength photodetector, and a Tektronix CSA 803 communications signal analyzer. Typical response profiles for a 100 x 5 μm device are shown in Fig. 1. The maximum current pulse achieved was about 80-90 mA limited by the 5V maximum amplitude of the pulse generator, the diode turn-on voltage, and a 33 Ω external series resistance. The resistance of the laser diode plus the external resistor was typically 36.5-38 ohms.

The variation of the square of the relaxation oscillation frequency with the bias current above threshold was determined for 50, 100, 200, and 400 μm long x 5 μm wide lasers from the 4 and 5QW GRINSCH wafers. The slope of the line fitted to each set of data was used to calculate the differential gain, dg/dn, of the various lasers according to the equation:

$$\frac{dg}{dn} = \frac{4\pi^2 eWdL}{\eta_i v_g \gamma} \frac{f_0^2}{(I - I_{th})} \tag{1}$$

where W is the ridge width, L is the cavity length, d is the active region thickness, η_i is the internal quantum efficiency, v_g is the group velocity, γ is the optical confinement factor, f_0 is the relaxation oscillation frequency, and $(I-I_{th})$ is the current level above threshold. Eqn. (1) is identical to that used by Eom[4], except that the internal quantum efficiency is included. The confinement factor was found using the effective index method, and the internal quantum efficiencies were determined to be 78% and 95% for the 4 and 5QW lasers, respectively. The latter calculation assumes a mirror reflectivity of 0.32, which is valid since the dry-etched and cleaved mirror lasers have such similar threshold currents[7]. The differential gain calculated according to eqn. 1 is plotted as a function of the cavity length for the 4 and 5QW GRINSCH material in Fig. 2. Contrary to theoretical predictions, the differential gain determined for the 5QW lasers is lower and varies much less than the values for lasers from the 4QW wafer. This result may be caused by partial relaxation of the highly strained material or uneven pumping of the widely separated quantum wells. The 4QW 400 μm long laser has a very high differential gain of 1.6×10^{-15} cm^2, but the very short cavity length 4QW devices have only about 50%-60% of this value due to gain saturation.

The lasers were then mounted p-side up on copper heat sinks, and the microwave modulation response was measured from 0.045 to 26.5 GHz with an HP 8510B network analyzer and the New Focus photodetector. An important consequence of reducing the cavity length to improve the bandwidth of a laser is the resultant increase in the threshold current density and device heating under cw operation. Whereas the resonance frequency for a 50 x 5 μm laser from the 5QW GRINSCH wafer increased linearly with current under pulsed conditions, the RF data in Fig. 3 shows a sub-linear response under cw conditions at currents greater than 10 mA above threshold ($1.5xI_{th}$). This behavior continues up to a current density of 16 kA/cm^2 beyond which the device usually fails due to excessive heating. As a result, the maximum resonance frequency under cw operation for the 50 μm long devices is about 16 GHz. This value is less than half of what was observed from the impulse response tests, in which an f_0 of 35 GHz was observed.

The microwave characteristics of 50 and 100 μm long by 5 μm wide 5QW GRINSCH lasers were tested to determine their respective 3-dB bandwidths and modulation efficiencies. Fig. 4

shows the modulation response of the same 50 x 5 μm device as in Fig. 3. The maximum 3-dB bandwidth of 22 GHz is the highest frequency response obtained for this wafer under cw operation. The low-frequency modulation efficiency drops about 7 dB between the 14.63 mA ($1.5xI_{th}$) and 40.93 mA ($4xI_{th}$) curves. Since the impedance of the device--laser plus parasitics--is constant with bias, this drop is believed to be caused primarily by the heating that is evident in fig. 3. Heating causes the modulation efficiency to decrease because of a reduction in the slope efficiency. In Fig. 5, the modulation response of a 100 x 5 μm laser with a maximum 3-dB bandwidth of 20 GHz is shown. The modulation efficiency drops only 0.5 dB compared to its low bias value. The excellent modulation efficiency over a wide bias range is attributed to the relatively constant impedance of the device and better heat-sinking of this particular laser. This result shows that strained-layer multiple quantum well lasers not only have high bandwidth but also outstanding modulation efficiency.

The cw operation of the 50 and 100 μm long 4QW GRINSCH lasers was not very reliable because of device heating. The reason for this dissimilarity compared to the 5QW wafer is believed to be the difference in substrate thickness. Though the 5QW wafer was thinned to about 60 μm, the 4QW wafer was polished to just 100 μm. The microwave modulation was measured under cw and pulsed bias (the latter with 2 μsec pulses, 13% duty cycle) to determine the effect of heating on the frequency response[21]. Under these conditions, typical maximum 3-dB bandwidths were 18 GHz cw, 21 GHz pulsed and 15 GHz cw, 20 GHz pulsed for 100 and 50 μm cavity length 4QW GRINSCH lasers, respectively.

Although heating limited the bandwidth of both the 4 and 5 QW GRINSCH lasers, the low frequency rolloff evident in the modulation response curves of Figs. 4 and 5 was another major problem. In contrast, the low frequency response of the 4QW SCH lasers was considerably better. In Fig. 6, the modulation response of a 100 x 3 μm 4QW SCH device is compared to that of a 100 x 3 μm 4QW GRINSCH laser. It is believed that the low frequency roll-off present in both devices is caused by the finite carrier capture time into the quantum wells and is characterized by a low pass filter of the form $1/(1 + \omega^2\tau_{cap}^2)$[17,18]. This topic will be discussed in detail in the next section. After examining Fig. 8 closely, it is clear that the SCH laser has better low frequency behavior than the GRINSCH laser. Capture times of 18 ps and 72 ps are calculated for the SCH and GRINSCH devices, respectively. This substantial difference in capture times can be explained by the possibility that electrons accelerated by the built-in electric field in the GRINSCH structure traverse the quantum well region without losing much energy and are trapped by the wells only after being redirected by the electric field on the opposite side the GRINSCH structure. In the SCH laser, electrons injected into the quantum well region can never overshoot this area because of the high energy barrier on the opposite side of the SCH. Thus, the SCH traps the electrons more quickly than the GRINSCH and has a faster capture time.

Maximum 3-dB modulation bandwidths of 15 and 25 GHz were measured on 50 and 100 μm 4QW SCH lasers, respectively. The best device was a 150 μm cavity length device that had a 3-db bandwidth of 28 GHz at a bias current of 105 mA, corresponding to an output power of about 40 mW. The modulation response of this device at various bias currents is shown in Fig. 7. The high-frequency performance of the 150 μm length laser benefits greatly from the improved low frequency behavior. As will be presented below, this 4QW SCH device also has significantly lower damping at high powers than any of the GRINSCH lasers. The performance of all these 4QW SCH devices is limited by degradation of the very narrow p-contact metallization at the large current densities (> 20 kA/cm^2) required to achieve high optical powers. Since the substrate was thinned to approximately 40 microns in thickness, heating of the device was not really a problem.

4. DAMPING AND LOW FREQUENCY RESPONSE IN QW LASERS

For a quantum well laser that has a finite carrier capture and emission time into and out of the well, the single mode rate equations have the following form[17,18] (ignoring non-linear gain saturation):

$$\frac{dN_b}{dt} = \frac{i}{e} - \frac{N_b}{\tau_s} - \frac{N_b}{\tau_{cap}} + \frac{N_w}{\tau_e} \tag{2}$$

$$\frac{dN_w}{dt} = \frac{N_b}{\tau_{cap}} - \frac{N_w}{\tau_e} - \frac{N_w}{\tau_s} - v_g GVS \tag{3}$$

$$\frac{dS}{dt} = \Gamma v_g GVS - \frac{S}{\tau_p} \tag{4}$$

where N_b is the number of carriers in the quantum well barrier, N_w is the number of carriers in the well, i is the injected current, S is the photon density, G is the material gain, V is the quantum well volume, Γ is the confinement factor, v_g is the group velocity, and τ_s, τ_{cap}, τ_e, and τ_p are the carrier recombination, capture, emission, and photon cavity lifetimes, respectively. Using a small signal analysis to evaluate (3)-(5), one obtains a relative modulation response function of the form:

$$|R|^2 = \frac{1}{1 + \omega^2\tau_{cap}^2} \frac{\omega_o^4}{(\omega^2 - \omega_o^2)^2 + \omega^2\gamma^2} \tag{5}$$

$$\omega_o^2 = \frac{v_g \frac{dG}{dN} S_o}{\tau_p \sigma} \tag{6}$$

$$\gamma = \frac{1}{\sigma\tau_s} + \frac{\omega_o^2\tau_p}{\sigma} + \frac{1}{\sigma\tau_e} \frac{\omega^2\tau_{cap}^2}{\left(1 + \omega^2\tau_{cap}^2\right)} \tag{7}$$

$$\sigma = 1 + \frac{\tau_{cap}/\tau_e}{(1 + \omega^2\tau_{cap}^2)} \tag{8}$$

Equation (5) reflects the standard damped resonance of an ideal laser, but the response is modified by the addition of a low pass filter. If $\omega^2\tau_{cap}^2 \ll 1$, then carrier transport effects can be interpreted as reducing the differential gain and the damping rate, γ, by the factor $\sigma = 1 + \tau_{cap}/\tau_e$. If $\omega^2\tau_{cap}^2 \gg 1$, which is the case for the GRINSCH lasers reported in this work, then σ and γ can be written as:

$$\sigma \cong 1 \tag{9}$$

$$\gamma \cong \frac{1}{\tau_s} + \omega_o^2\tau_p + \frac{1}{\tau_e} \tag{10}$$

For this approximation to hold well, τ_{cap} should also be less than τ_e. As one can see from (9) and (10), a significant increase in damping can occur for $\tau_e \cong 100$ ps, but the effective reduction in differential gain is minimal. Fig. 8 shows a plot of the damping rate as a function of the square of the resonance frequency for 50-100 μm cavity length devices from the 4 and 5QW GRINSCH wafers. Since the damping rate does not always obey a model that assumes γ is linear with photon density, the characterization of the damping through the use of the so-called K-factor and the non-linear gain suppression coefficient, ε, will be avoided. From f_o^2 = 0-200 GHz^2, the damping rate presented in Fig. 8 is nearly constant. Above f_o^2 = 200 GHz^2, γ increases linearly, which is indicative of non-linear gain saturation at high photon densities. At low f_o^2, the damping rate is 10-15 GHz^2, which is much larger than $1/\tau_s$ (typically 1-2 GHz). Therefore, assuming that $\gamma \cong 1/\tau_e$, emission times of 100 ps and 67 ps are calculated for the 4 and 5QW GRINSCH lasers, respectively. The damping rate of the 28 GHz bandwidth 150 μm 4QW SCH laser has been included in Fig. 8 for comparison. In this device, γ is somewhat less at low f_o^2 and follows the same trend as the GRINSCH lasers up to about f_o^2 = 250 GHz^2. At high f_o^2, however, γ is much less than in any of the GRINSCH lasers. This improvement could be a result of the laser operating in a single longitudinal or lateral mode at high optical powers, whereas the other lasers experience mode competition.

Since the condition $\omega^2\tau_{cap}^2 \ll 1$ applies to the 4QW SCH lasers (τ_{cap} = 18 ps), the reduction in the differential gain due to carrier transport can be estimated as long as one assumes that 100 μm cavity length 4QW SCH and GRINSCH devices have the same τ_e--100 ps. A value of 1.18 is computed using $\sigma = 1 + \tau_{cap}/\tau_e$. An average value of 8.25 x 10^{-16} cm^2 was calculated for the differential gain of the 100 μm long SCH lasers. Multiplying this number by 1.18 gives an "intrinsic" dg/dn of 9.7 x 10^{-16} cm^2, which is fairly close to the 1.04 x 10^{-15} cm^2 differential gain found in Fig. 2 for the 100 μm 4QW GRINSCH lasers.

5. CONCLUSION

Strained-layer 4QW $In_{0.3}Ga_{0.7}As$ GRINSCH lasers with 400 μm cavity length fabricated by CAIBE have shown differential gain values approximately five times greater than those of high-frequency p-typed doped InGaAsP lasers[4]. Saturation of the optical gain in 50-100 μm devices limits the differential gain to between 8-10 x 10^{-16} cm^2. 5QW strained-layer GRINSCH lasers appear to suffer from either partial relaxation of the gain medium or uneven pumping of the quantum wells. Nevertheless, a CW 3-dB bandwidth of 22 GHz has been measured on a 50 μm long 5QW GRINSCH laser limited by both heating and a substantial low frequency rolloff. Significant improvement in this low pass filter effect has been achieved by employing an SCH structure rather than a GRINSCH. As a result, a record 3-dB bandwidth of 28 GHz has been demonstrated in a 150 μm long 4QW SCH laser. Finally, it has been shown that a carrier transport

model can accurately simulate both the low pass filter and damping behavior of quantum well lasers. This theory allows the extraction of both the carrier capture and emission times under certain optimum conditions.

ACKNOWLEDGMENT

The authors would like to thank John Johnson and George Porkolab for numerous discussions and processing tips about CAIBE and Kerry Litvin for expert opinions on microwave measurements. In addition, the authors greatly appreciate the assistance of Prof. R. C. Compton and Dr. L. Rathbun in using the Tektronix oscilloscope and Prof. N. MacDonald and E. Santos for use of their high-speed pulse generator. This work was primarily supported by ONR under contract # N00014-89-J-1386 with additional support from GE, IBM, and DARPA.

REFERENCES

[1] Suemune, L. A. Coldren, M. Yamanishi, and Y. Kan, "Extremely wide modulation bandwidth in a low threshold current strained quantum well laser," Appl. Phys. Lett., vol. 53, pp. 1378-1380, 1988.

[2] S. D. Offsey, W. J. Schaff, P. J. Tasker, and L. F. Eastman, "Optical and microwave performance of GaAs-AlGaAs and strained layer InGaAs-GaAs-AlGaAs graded index separate confinement heterostructure single quantum well lasers," IEEE Photon. Technol. Lett., vol. 2, pp.9-11, 1990.

[3] L. F. Lester, S. D. Offsey, B. K. Ridley, W. J. Schaff, B. A. Foreman, and L. F. Eastman, "Comparison of the theroetical and experimnetal differential gain in strained layer InGaAs/GaAs quantum well lasers," Appl. Phys. Lett., vol. 59, pp. 1162-1164, 1991.

[4] J. Eom, C. B. Su, J. S. LaCourse, and R. B. Lauer, "The relation of doping Level to K factor and the effect of ultimate modulation performance of semiconductor lasers," IEEE Photon. Technol. Lett., vol. 2, pp. 692-694, 1990.

[5] S. D. Offsey, L. F. Lester, W. J. Schaff, and L. F. Eastman, "High-speed modulation of strained-layer InGaAs-GaAs-AlGaAs ridge waveguide multiple quantum well lasers," Appl. Phys. Lett., vol. 58, pp. 2336-2338, 1991.

[6] R. Nagarajan, T. Fukushima, J. E. Bowers, R. S. Geels, and L. A. Coldren, "High-speed InGaAs/GaAs strained multiple quantum well lasers with low damping," Appl. Phys. Lett., vol. 58, pp. 2326-2328, 1991.

[7] L. F. Lester, W. J. Schaff, X. Song, and L. F. Eastman, "Optical and RF characteristics of short cavity length multiquantum well strained layer lasers," IEEE Photon. Technol. Lett., vol. 3, pp. 1049-1051, 1991.

[8] Y. Hirayama, M. Morinaga, N. Suzuki, and M. Nakamura, "Extremely reduced nonlinear K-factor in High-speed strained layer multiquantum well DFB lasers," Electron. Lett., vol. 27, pp. 875-876, 1991.

[9] P. J. A. Thijs, L. F. Tiemeijer, P. I. Kuindersma, J. J. M. Binsma, and T. Van Dongen, "High-performance 1.5 μm wavelength InGaAs-InGaAsP Strained Quantum Well Lasers and Amplifiers," IEEE J. Quantum Electron., vol. QE-27, pp. 1426-1439, 1991.

[10] R. Nagarajan, T. Fukushima, J. E. Bowers, R. S. Geels, L. A. Coldren, "Single quantum well strained InGaAs/GaAs lasers with large modulation bandwidth and low damping," Electron. Lett., vol. 27, pp. 1058-1060, 1991.

[11] W. F. Sharfin, J. Schlafer, W. Rideout, B. Elman, R. B. Lauer, J. LaCourse, and F. D. Crawford, "Anomalously High Damping in Strained InGaAs-GaAs Single Quantum Well Lasers," IEEE Photon. Technol. Lett., vol. 3, pp. 193-195, 1991.

[12] N. K. Dutta, J. Lopata, D. L. Sivco, and A. Y. Cho, "High-speed modulation and nonlinear damping effect in InGaAs/GaAs lasers," J. Appl. Phys, vol. 70, pp. 2476-2478, 1991.
[13] L. D. Westbrook, N. C. Fletcher, D. M. Cooper, M. Stevenson, P. C. Spurdens, "Intensity noise in 1.5 μm GaInAs quantum well buried heterostructure laser," Electron. Lett., vol. 25, pp. 1183-1184, 1989.
[14] M. Cavelier, J.-M. Lourtioz, J.-M. Xie, L. Chusseau, B. De Cremoux, M. Krawkovski, and D. Rondi, "Gain compression and phase-amplitude coupling in GaInAs quantum well lasers with three, five and seven wells," Electron. Lett., vol. 27, pp. 513-515, 1991.
[15] M. Willatzen, A. Uskov, J. Mork, H. Olesen, B. Tromborg, and A.-P. Jauho, "Nonlinear gain suppression in semiconductor lasers due to carrier heating," IEEE Photon. Technol. Lett., vol. 3, pp. 606-609, 1991.
[16] T. Takahashi and Y Arakawa, "Nonlinear gain effects on spectral dynamics in quantum well lasers," IEEE Photon. Technol. Lett., vol. 3, pp. 106-107, 1991.
[17] W. Rideout, W. F. Sharfin, E. S. Koteles, M. O. Vassell, and B. Elman, "Well-barrier hole burning in quantum well lasers," IEEE Photon. Technol. Lett., vol. 3, pp. 784-786, 1991.
[18] R. Nagarajan, T. Fukushima, S. W. Corzine, and J. E. Bowers,"Effects of carrier transport on high-speed quantum well lasers," Appl. Phys. Lett., vol. 59, pp. 1835-1837, 1991.
[19] K. Uomi, N. Chinone, T. Ohtoshi, and T. Kajimura, "High relaxation oscillation frequency (beyond 10 GHz) of GaAlAs multiquantum well lasers," Japan. J. Appl. Phys., vol. 24, pp. L539-L541, 1985.
[20] L. F. Lester, W. J. Schaff, S. D. Offsey, and L. F. Eastman, "High-speed modulation of InGaAs-GaAs strained-layer multiple-quantum-well lasers fabricated by chemically assisted ion-beam etching," IEEE Photon. Technol. Lett., vol. 3, pp. 403-405, 1991.
[21] J. E. Bowers, B. R. Hemenway, A. H. Gnauck, and D. P. Wilt, "High-Speed InGaAsP Constricted-Mesa Lasers," IEEE J. Quantum Electron., vol. QE-22, pp.833-844, 1986.

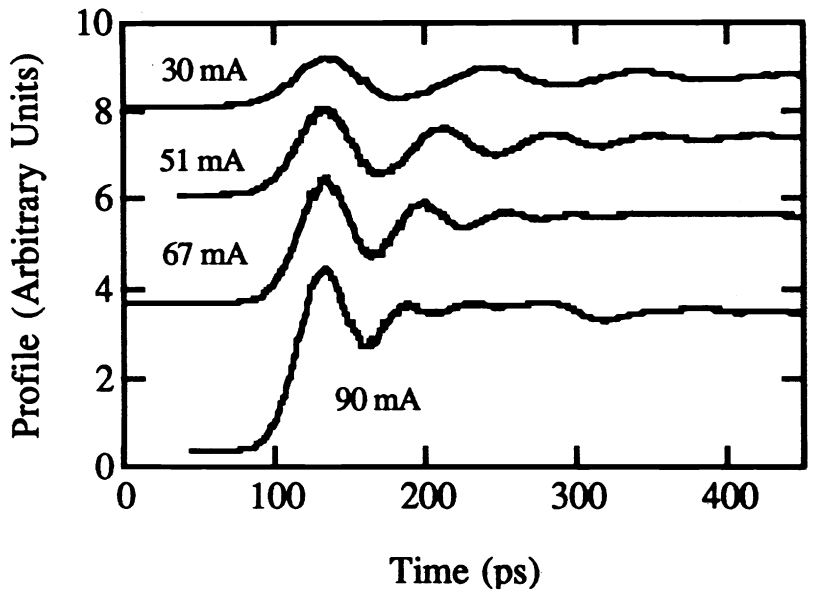

Fig. 1. Relaxation oscillation profiles of a 100 x 5 μm 4QW GRINSCH laser. The time interval between the second and third peaks of the 90 mA curve is 42.5 ps (23.5 GHz).

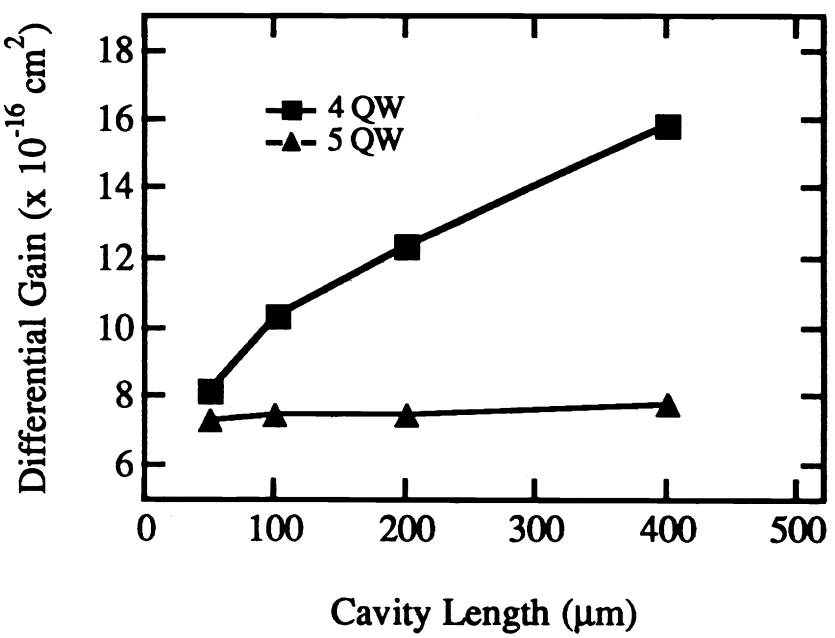

Fig. 2. The calculated differential gain as a function of cavity length. dg/dn decreases only slightly with length for the 5QW GRINSCH lasers, but decreases over 90% for the 4QW GRINSCH devices

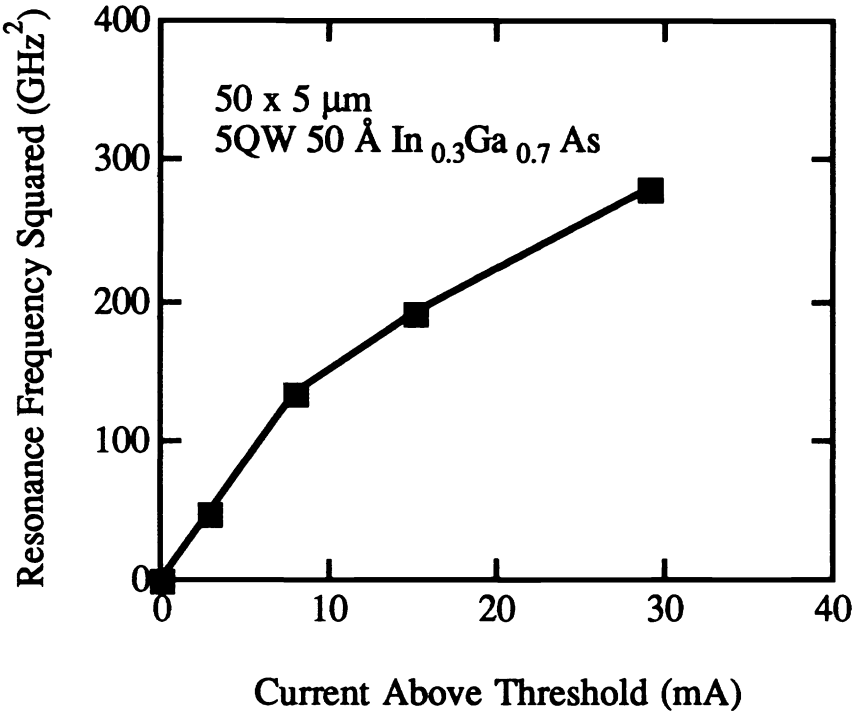

Fig. 3. The variation of the resonance frequency squared with $(I - I_{th})$ is quite sub-linear for a 50 x 5μm 5QW GRINSCH laser operated cw and mounted p-side up.

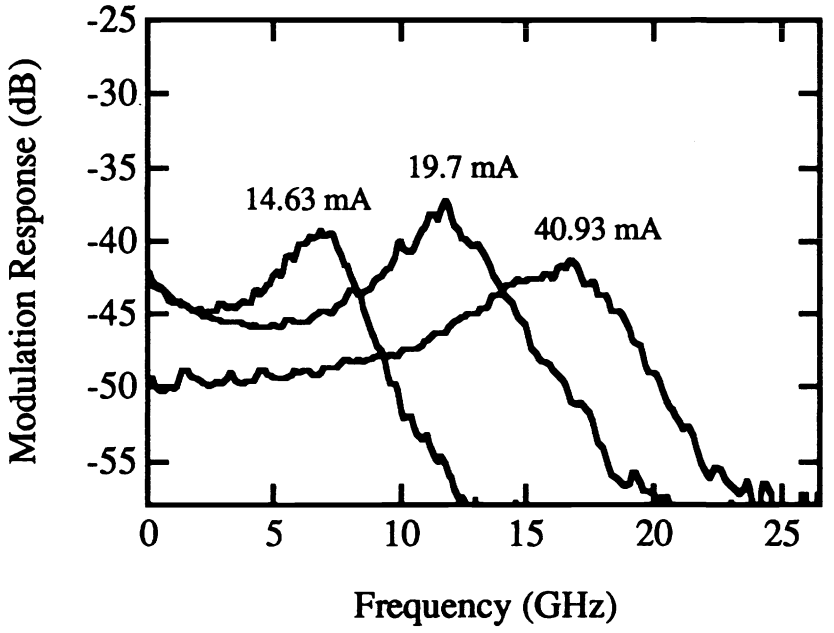

Fig. 4. The modulation response of a cw operated 50 x 5 μm 5QW GRINSCH laser for three different bias levels. The effect of heating is evident in the warped curve at 40.93 mA bias. The maximum 3-dB bandwidth of this laser is 22 GHz.

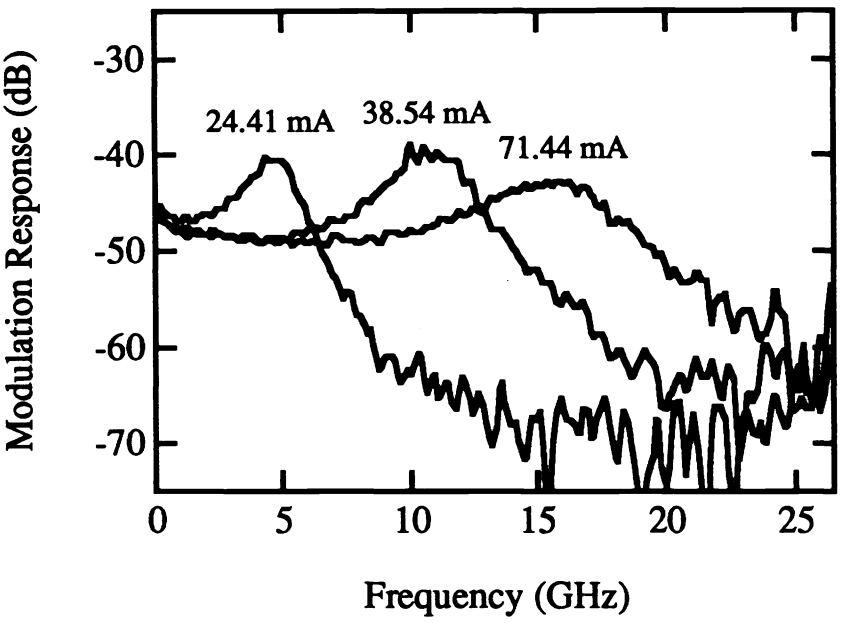

Fig. 5. A 100 x 5 μm 5QW GRINSCH laser showing excellent modulation efficiency and a maximum 3-dB bandwidth of 20 GHz. The drop in modulation efficiency is only 0.5 dB compared to its low-frequency, low-bias value.

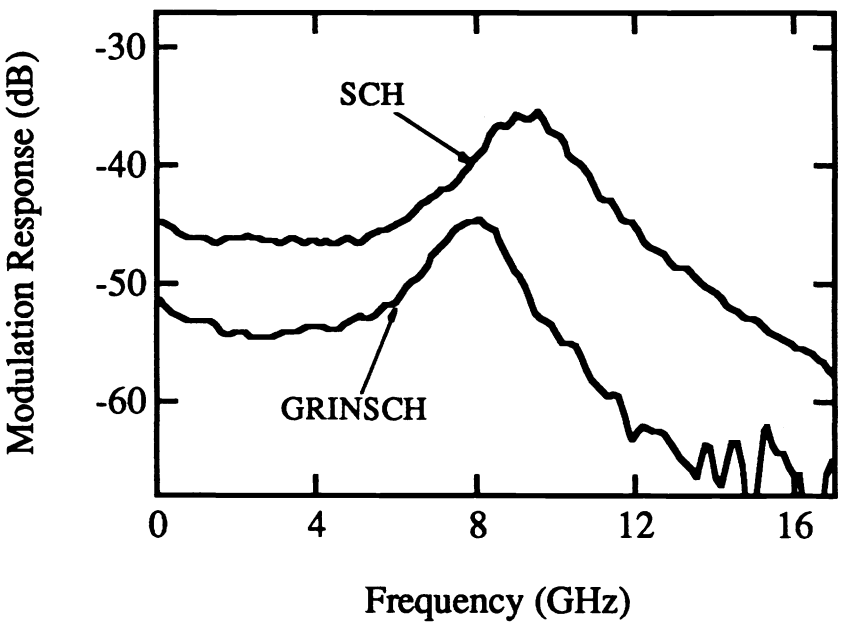

Fig. 6. A comparison of the modulation responses of the 4QW GRINSCH and SCH 100 x 3 μm lasers at current bias of about 21 mA. Below 4 GHz, the GRINSCH laser has noticeably more rolloff than the SCH device.

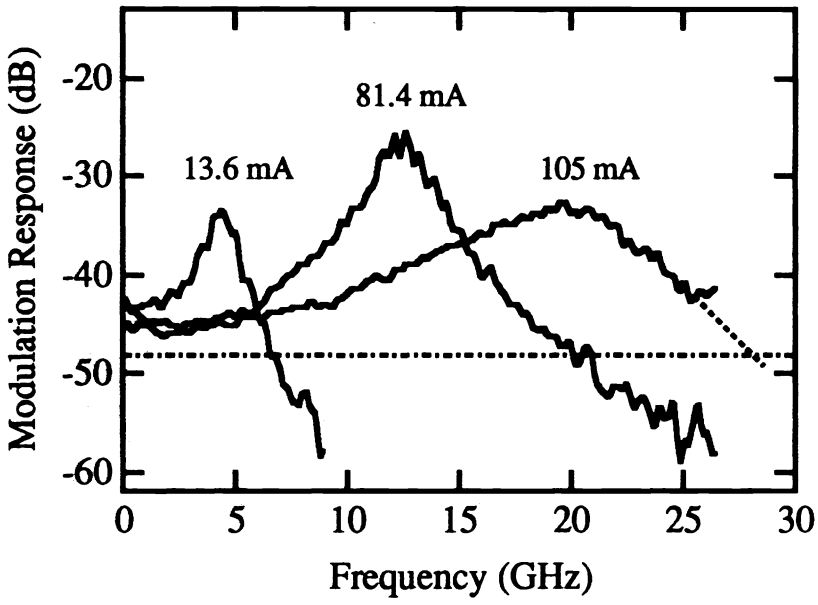

Fig. 7. The CW modulation response of the 150 μm 4QW SCH strained-layer laser at various bias currents. The dot-dashed line is 3-dB below the DC level of the 105 mA curve. The 0-dB bandwidth is 26.5 GHz and the 3-dB bandwidth is found by extrapolation to be 28 GHz.

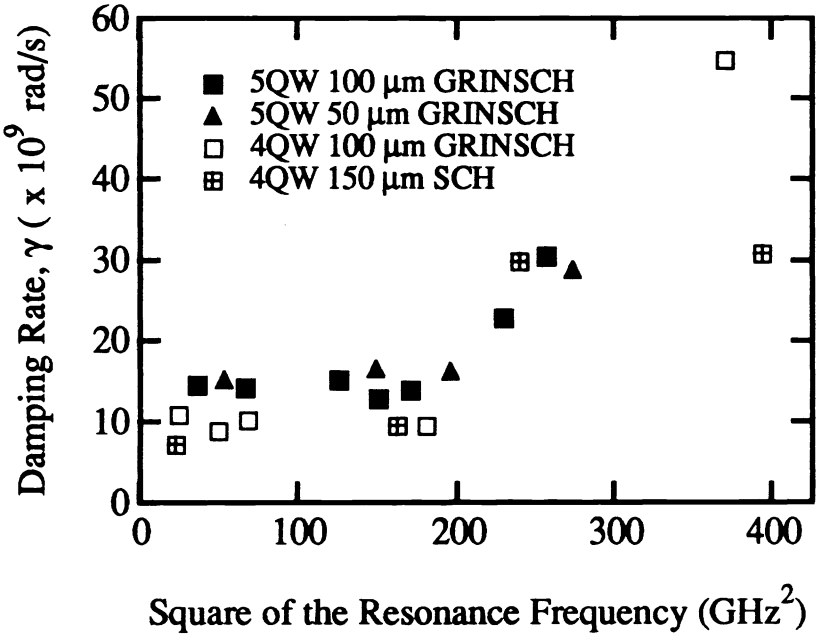

Fig. 8. A graph of the damping rate as a function of the square of the resonance frequency for various short cavity GRINSCH lasers and the high bandwidth 4QW SCH laser.